Short communication

Sol–gel based silica electrodes for inorganic membrane direct methanol fuel cells

Hyea Kim, Paul A. Kohl*

School of Chemical and Biomolecular Engineering, Georgia Institute of Technology, 311 Ferst Dr., Atlanta, GA 30332-0100, United States

ABSTRACT

Inorganic glass electrodes are of interest for use with inorganic proton exchange membranes for direct methanol fuel cells. Platinum–ruthenium glass electrodes (PtRu/C-SiO$_2$) have been prepared by incorporating the PtRu/C nanoparticles into a silica-based matrix. The SiO$_2$ matrix was synthesized through the sol–gel reaction of 3-(trihydroxysilyl)-1-propanesulfonic acid (3TPS) and 3-glycidoxypropyltrimethoxysilane (GPTMS). The distribution of the PtRu/C particles can be controlled by changing the properties of the gel matrix. The effect of gelation time, mole fraction of reactants within the sol, curing temperature, and glass ionomer content were investigated. The adhesion of the catalyst layer on the membrane, catalytic activity for methanol oxidation, and inhibition of methanol permeation through the membrane have been characterized and optimized. The electroless deposition of PtRu onto the PtRu/C nanoparticles was performed to increase the sheet conductivity of the electrode. It was found that the electrolessly deposited metal improved the catalytic activity for methanol oxidation and decreased the methanol cross-over. The methanol fuel cell performance using the inorganic membrane electrode assembly was 236 μA cm^{-2} at 0.4 V and was stable for more than 10 days.

© 2009 Elsevier B.V. All rights reserved.

1. Introduction

Direct methanol fuel cells (DMFCs) have attractive cost and energy-density features especially for portable, low-power electronic devices (μW to mW), such as wireless sensors. The high energy density of DMFCs results in small volume cells, if compact, low cross-over membranes can be produced. Passive DMFC system, which operates at atmospheric temperature and pressure, are simple designs with minimal balance of plant. Stand-alone, passive DMFCs face several challenges including reducing the fuel loss through methanol cross-over, orientation-independent operation, and development of a carbon dioxide vent for discharge of carbon dioxide from the fuel tank [1–3]. High methanol permeability is the most critical challenge to obtain long-life cells [4]. Methanol cross-over reduces the cathode performance and lowers the fuel efficiency, which limits the life time of the fuel cell. Methanol permeability can be severe with passive fuel-delivery systems because the fuel is always in contact with the membrane resulting in lower current density and open-circuit voltage (OCV) compared to an active fuel-delivery system [5].

Several studies have investigated approaches to lower the methanol cross-over. Two approaches have been taken. First, traditional, perfluorinated polymer membranes have been modified by inclusion of inorganic fillers to produce Nafion composite

membranes [6,7]. Second, new membrane materials have been developed, such as those formed from inorganic silica materials [8,9]. Prakash et al. fabricated phosphorous-doped silicate glass (PSG) membranes by plasma enhanced chemical vapor deposition (PECVD) and showed that the PSG can be used as a proton exchange membrane for low-power applications [10]. Nogami and co-workers have synthesized proton conducting silicate glasses via sol–gel reaction [11–14]. In order to generate ionic-conducting defects during the sol–gel reaction, a second precursor, such as phosphorous ions, was introduced into the silicon dioxide matrix. The silica matrix was composed of tetraortho silicate (TEOS). In addition, functionalized silanes were used to create sulfonic acid-functionalized silica proton conductive membranes [15]. The methanol permeability coefficient of the functionalized glass membrane was 2.17×10^{-9} mol cm cm^{-2} day^{-1} Pa^{-1}, which was three orders of magnitude less than Nafion. The membrane had a moderate ionic conductivity of 3×10^{-3} S cm^{-1}.

Although the efficiency of the DMFC was improved due to the methanol permeability of the glass vs. polymer membrane [15], the stability of the glass-based direct methanol cell performance was not adequate because a traditional polymer-based catalyst was used with the glass membranes. Using a different ionomer materials in the catalyst layer from the membrane itself causes several problems. For example, the contact resistance between the glass membrane and the electrodes is likely to be lowered if the materials are more compatible. The coefficient of thermal expansion of the polymer-based electrodes is significantly different from the glass electrolyte, putting the long term stability into question. Further,
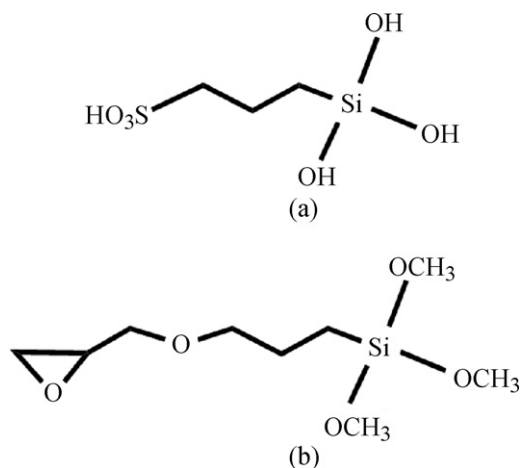

Fig. 1. The chemical structure of (a) 3TPS, and (b) GPTMS.

using a water-rich polymer ionomer in the catalyst layer is a reliability concern, since the catalyst structure is soaked for long periods in aqueous methanol. The polymer-based ionomer could swell and change the catalyst structure resulting in loss of the three phase boundary, which is a key parameter to achieve high performance. Therefore, it is important to develop glass-based electrodes for use with glass membranes in fabricating polymer-free membrane electrode assemblies (MEA).

In previous studies, we have focused on developing Pt/C-SiO$_2$ composite electrodes [16]. The Pt/C nanoparticles were incorporated into a porous silicon dioxide glass matrix synthesized from TEOS through a sol–gel reaction. The electroless platinum deposition used an acidic Leaman bath [17,18] to increase the sheet conductivity of the Pt/C-SiO$_2$ composite electrodes. Further, the Pt/Ru catalyst was electrolessly deposited in an acidic bath and was shown to be an effective surface for methanol oxidation [19].

In this report, improvements to the PtRu/C-SiO$_2$ composite glass electrodes, including conductivity, are presented. The electrodes were synthesized from sulfonic acid-functionalized silica prepared using 3-(trihydroxysilyl)-1-propanesulfonic acid (3TPS) and 3-glycidoxypropyl trimethoxysilane (GPTMS). 3-(Trihydroxysilyl)-1-propanesulfonic acid (3TPS) has been studied, due to its similarity with 3-mercaptopropyl trimethoxysilane (3MPS) in the membrane [15]. The structure of 3TPS is shown in Fig. 1. The sulfonic acid group in 3TPS provides proton conductivity in the catalyst layer. The three hydroxyl groups of the 3TPS can react with water and condense to form a silica matrix including encapsulation of the catalyst in the matrix. The epoxy content of the GPTMS improved the mechanical properties and provided cross-linking in the silicon dioxide matrix and the catalyst activity for methanol oxidation has been improved. The methanol permeation has been reduced by increasing the catalyst density in the electrode.

2. Experimental

The PtRu/C-SiO$_2$ electrodes were prepared by incorporating commercial PtRu/C catalysts into a silicon dioxide glass matrix. The PtRu/C catalyst (E-TEK) was 60 wt% metal loading and 1:1 atomic ratio of Pt and Ru. The glass matrix for the catalyst layer was made via the reaction of 3TPS and GPTMS (Gelest Corporation). The mole percent of 3TPS-to-GPTMS was varied from 0, 50, 83, 90 to 95%. Four milliliter of methanol and 3 drops of HCl were added to 5 mL of the sol mixture. No water for the sol–gel reaction was added, since the 3TPS was obtained as an aqueous form with twentyfold excess water (by mole ratio). After reacting the sol for different gelation times (1–24 h), the gel solutions and PtRu/C were combined

and mixed for 1 h. The weight ratio of PtRu/C catalyst-to-glass was varied from 2 to 7, while maintaining the same PtRu/C loading in the electrodes (2 mg PtRu cm^{-2}). The catalyst and gel mixture were brush-painted on the membrane and cured at 80 °C for 12 h.

The electroless deposition of the PtRu films was carried out on PtRu/C-SiO$_2$ electrodes in a modified acidic Leaman bath [17,18]. The Pt/Ru electroless bath contained 3.3 g 100 mL^{-1} of HCl, 0.2 g 100 mL^{-1} of 5-sulfosalycylic acid hydrate (Sigma–Aldrich), 0.05 g 100 mL^{-1} of 1,3,6 sodium naphthalene trisulfonate tribasic hydrate (Sigma–Aldrich), and 0.06 g 100 mL^{-1} of benzene 1,3 disulfonate (Sigma–Aldrich). The reducing agent was formic acid (1 g 100 mL^{-1}). Hexachloroplatinic acid and ruthenium (III) chloride were used as the source of Pt and Ru ions, respectively. The preparation and characterization of the electrolessly deposited PtRu bimetal has been described in the previous publication [19]. The electroless deposition of Pt for the cathode electrode was performed using the original Leaman bath with hydrazine dihydrochloride as a reducing agent. The Pt bath temperature was 70 °C and the deposition time was 30 min.

The electrochemical experiments were performed with a PARSTAT 2263 (Princeton Applied Research) potentiostat. Linear sweep voltammogram (LSV) was carried out in a three-electrode cell. Glass-based electrodes were fabricated on carbon paper and used as the working electrode with platinum foil (Sigma–Aldrich) as the counter electrode and a saturated calomel (SCE) reference electrode (CH Instruments). The voltammograms were obtained in an aqueous 0.5 M H$_2$SO$_4$, 1 M methanol solution. The potential sweep was repeated at least 10 times between −0.4 and 1.5 V vs. SCE. The scan rate was 10 mV s^{-1}.

Adhesion of the composite electrode on the glass proton exchange membrane was evaluated by soaking the electrode/membrane structure in 1:1 vol% of water and methanol solution, and ultrasonicated for 1 h at room temperature. The weight loss of the electrode by ultrasonic vibration was measured. Methanol permeability of the bare membrane and MEA was determined by sealing the membrane to the open end of a methanol-filled vial. The loss of methanol was determined gravimetrically. The permeability coefficient was calculated using Eq. (1).

$$P = \frac{N \times \delta}{\Delta P \times A} \tag{1}$$

where P is the permeability coefficient of the membrane, ΔP is the pressure drop across the membrane, A is the exposed membrane area available for fuel transport through the membrane, δ is the electrolyte thickness, and N is the number of moles lost by permeation. The relative error in the permeability coefficient was less than 2%. The relative methanol permeability was calculated by comparing the permeability coefficients between the bare membrane and the same membrane with one electrode fabricated on it. The thickness of the membranes, with or without electrodes, was measured at five points and the average value is reported.

Impedance spectroscopy experiments were performed with a PerkinElmer PARSTAT 2263 potentiostat. The membrane was placed between the two glass cells and filled with 1.0 M H$_2$SO$_4$ electrolyte. A platinum electrode was placed on each side of the membrane at a fixed distance from the membrane and connected to a potentiostat. The frequency of the impedance measurements ranged from 100 mHz to 1 MHz with an AC signal amplitude of 10 mV. The relative error in the conductivity measurements was about 0.2%, which was insignificant.

Fuel cells were prepared with the sol–gel based sulfonic acid-functionalized glass membrane. The synthesis and optimization process of the glass membrane has been described previously [15]. The PtRu/C-SiO$_2$ and Pt/C-SiO$_2$ catalysts were painted on the anode and the cathode, respectively. After curing both electrodes

Table 1
The glass electrode thickness depending on the sol–gel reaction time.

Reaction time (h)	Thickness (μm)
1	7.8
3	9.5
6	12.5
9	16.8
12	24.5
24	32.6

at 80 °C for 12 h, the PtRu and Pt were electrolessly deposited on the anode and cathode, respectively. The linear polarization curves were obtained at a scan rate of 1 mV s^{-1}.

3. Results and discussion

The first step in the formation of a sol–gel based electrode is the creation of a stable, crack-free glass ionomer film, which can be loaded with metal catalyst and fabricated on the free-standing glass membrane. The glass ionomer was prepared via a sol–gel reaction with a 1:1 mole ratio of 3TPS-to-GPTMS. A fourfold excess of methanol by volume was added to the silane to make the mixture miscible. The excess methanol also slowed the rate of sol–gel condensation. If the sol–gel reaction occurred too quickly, the heat generated from the reaction caused the temperature to rise which accelerated the condensation reaction rate resulting in cracks in the glass films. The PtRu/C nanoparticles were incorporated under stirring into the gel mixture for 1 h, described above, and painted onto the membrane surface. Uniform thickness glass electrode was formed on the membrane surface by curing the PtRu/C-SiO$_2$ gel on the membrane at 50 °C for 12 h.

The effect of sol–gel reaction time (gelation time) on the formation of a composite PtRu/C-SiO$_2$ film was investigated. Table 1 shows the glass electrode thickness depends on function of gelation time. The thickness of the catalyst layer increased from 7.8 to 32.6 μm, when the gelation time increased from 1 to 24 h. The longer reaction time led to larger sol particles and the gel was more viscous, however, cracks were observed for reaction time greater than 6 h.

The crack formation in the glass electrode also affected the methanol permeability through the MEA. Fig. 2 shows the effect of gelation time on methanol permeability in the PtRu/C-SiO$_2$ catalyst layer. The additional glass layer in the electrode is expected
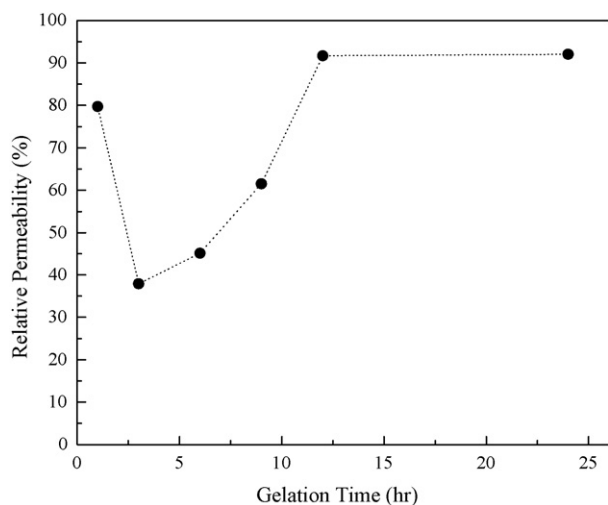
Fig. 2. The relative permeability of the one-side MEA to that of the bare membrane as a function of gelation time.
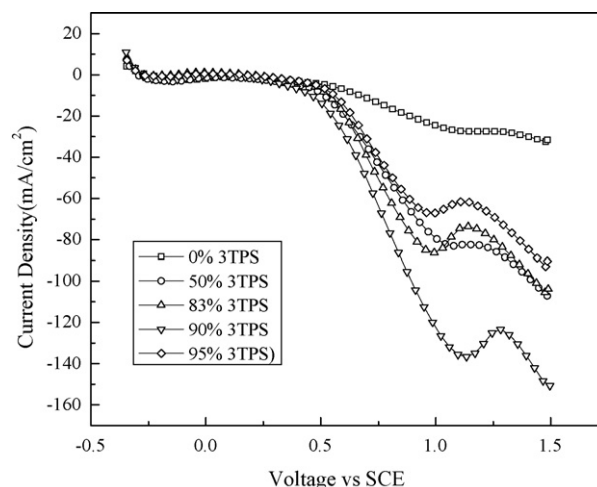
Fig. 3. Linear sweep voltammograms for different ionomer composition electrodes between 3TPS and GPTMS in 0.5 M H$_2$SO$_4$ and 1 M methanol, 1 cm^2, 23 °C, 50 mV s^{-1}.

to decrease the overall methanol permeability. The methanol permeability of a bare membrane was compared to one where one electrode was fabricated on one side of the membrane. When the sol–gel reaction time was increased to 3 h, the relative permeability was dropped by 62.1%. As the gelation time increased, the larger sol–gel particles resulted in less free volume in the electrode structure. However, the relative permeability was increased when the reaction time was longer than 6 h. The cracks in the electrode film provided an easy pathway for methanol permeation. After 12 h reaction time, the permeability was similar to that of the bare membrane. That is, the electrode structure offered little resistance to methanol permeation due to the severe formation of the cracks.

The effect of the 3TPS-to-GPTMS ratio was also investigated since they serve different functions within the sol–gel film. 3TPS provides the conductive, sulfonic acid moieties necessary for proton conductivity, and GPTMS provides epoxy cross-linking groups which enhance the mechanical strength of the catalyst layer and adhesion to the membrane. A higher mole fraction of 3TPS could increase the ionic conductivity, but may result in higher water adsorption and poor mechanical properties.

The electrode activity of the catalyst on the membrane was investigated in an aqueous 0.5 M H$_2$SO$_4$/1 M methanol solution. Fig. 3 shows the LSV of the PtRu/C-SiO$_2$ electrodes with different ionomer compositions. The mole ratio of 3TPS-to-GPTMS was increased from 0 to 95%. The peak current increased with 3TPS content. The ionic conductivity of the ionomer was higher due to the higher sulfonic acid content. The maximum current density was −140 mA cm^{-2} obtained with the 90 mol% 3TPS electrode (10 mol% GPTMS). This corresponds to 42,000 mA g^{-1} of PtRu/C catalyst, when the 3TPS was increased to 95 mol%, the current was lowered because there was an insufficient amount of GPTMS to provide adequate adhesion of the electrode on the membrane. In this case, some of the catalyst nanoparticles fell off the membrane surface.

In order to improve the adhesion of the glass electrode to the membrane, the PtRu/C-SiO$_2$ electrode was cured at a higher temperature, 100 °C. The samples with different ionomer contents were soaked in the methanol/water solution (1:1 volume ratio), and ultrasonicated for 1 h. The weight of the electrode was measured before and after sonication. During the sonication, some of the catalyst layer flaked off the surface when the electrode adhesion was poor. Fig. 4 shows the fraction of the electrode weight remaining on the membrane as a function of the ionomer composition and cure temperature. Increasing the GPTMS content led to a higher catalyst content at both temperatures. The remaining weight of the samples
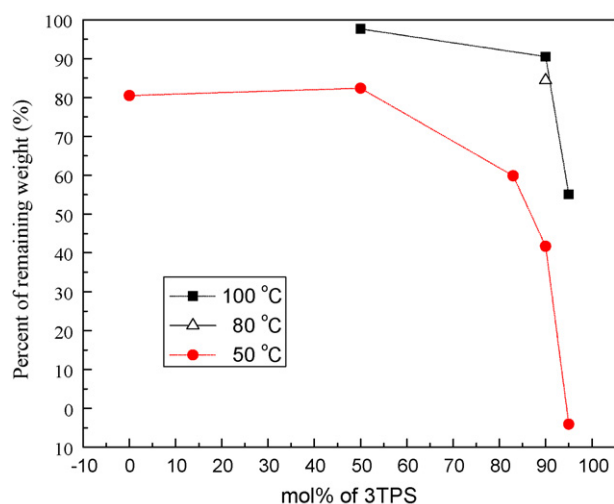
Fig. 4. Percent of remaining weight of the electrode after ultrasonicating for an hour in methanol and water solution as a function of the curing temperature (50, 80 and 100 °C) and different ionomer compositions.

cured at 100 °C was higher than that of the samples cured at 50 °C due to a larger extent of reaction in the electrode layer.

Although the adhesion of the glass electrodes on the membrane was improved by curing at 100 °C, the sulfonic acid moiety was not stable at this temperature. The conductivity of the membrane decreased after curing at 100 °C. The loss of conductivity is attributed to the fact that the –SO$_3$H groups may react with the –OH groups to form –S–O–C bridges and water at high temperatures [20,21]. Thus, the cure temperature was reduced to 80 °C where the conductivity remained essentially constant. One can see in Fig. 4 that for the 90% 3TPS sample the adhesion at 80 °C was much better than that at 50 °C. The remaining experiments were performed using membranes and electrodes with 90% 3TPS, allowed to gel for 3 h, and cured at 80 °C.

The ratio of catalyst-to-glass ionomer was investigated, since it is highly desirable to have adequate sheet conductivity within the electrode and the correct three-phase boundary needs to be established [22,23]. Higher PtRu/C loadings generally result in higher electrochemical surface area and electrode activity. However, insufficient glass ionomer can lead to poor encapsulation and adhesion of the catalyst particles. Fig. 5 shows that the relative methanol permeability and the sheet resistivity as a function of the catalyst-to-glass ratio. The relative permeability decreased significantly from 78.0 to 28.8% when the catalyst-to-glass ratio increased
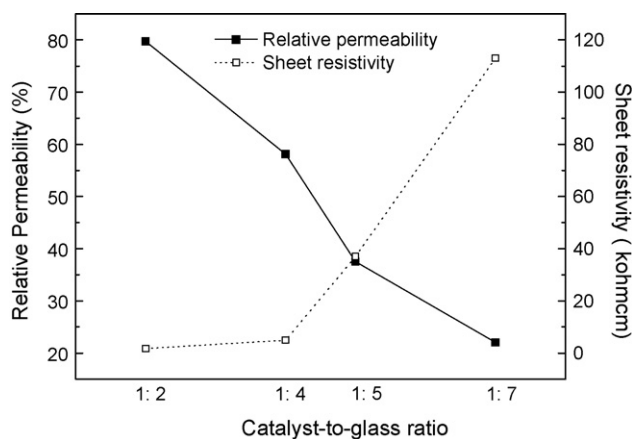

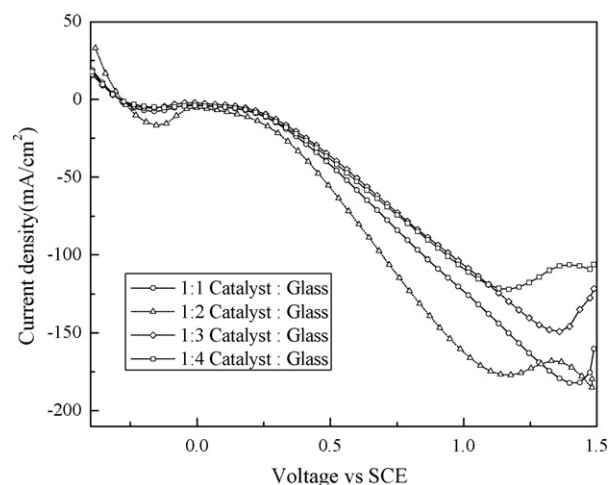**Fig. 5.** Relative permeability and sheet resistivity as a function of the glass ratio to catalyst.

Fig. 6. Linear sweep voltammograms for different ratios of catalyst-to-glass electrodes in 0.5 M H$_2$SO$_4$ and 1 M methanol, 1 cm^2, 23 °C, 50 mV s^{-1}.

from 2 to 7. The excess glass in the catalyst layer assisted in blocking methanol cross-over. The sheet resistivity was 1.7 kΩ cm when the catalyst-to-glass ratio was 2, however, it increased to 113 kΩ cm when the ratio was increased to 7. Although the glass ionomer was ionically conductive by virtue of the sulfonic acid content, the electrical resistance was high because it comes only from catalyst-to-catalyst contact.

The electrochemical activity of the composite catalyst with different catalyst-to-glass ratios was evaluated by performing linear sweep voltammetry from negative to positive voltages, as shown in Fig. 6. The electrode with a 1:2 catalyst-to-glass ratio provided the highest activity (highest current) in methanol in a potential range between 0.2 and 0.5 V vs. SCE. The 1:1 catalyst-to-glass sample had a higher metal content, however, the catalyst adhesion was poor and some of the catalyst particles flaked off the surface during use resulting in lower performance.

In order to decrease the sheet resistance by connecting the metal particles embedded in the glass ionomer, PtRu catalyst was electrolessly deposited onto the sol–gel fabricated electrode containing PtRu/C by using a modified acidic Leaman bath [19]. As the metal islands grow, the void spaces between PtRu/C particles are reduced and the electrochemical area changes. Initially, the active area increases as PtRu/C islands merge together and the sheet resistivity drops. Once the islands have merged together, additional deposition yields larger particles but may not yield an increase in real surface area or electrochemical activity.

The catalyst-to-glass ratio in the PtRu/C-SiO$_2$ composite catalyst might affect the PtRu electroless deposition. The sheet resistivity was measured as a function of the deposition time for the samples prepared at different catalyst-to-glass ratio from 2 to 7. Table 2 shows that the resistivity decreased with deposition time. At a given deposition time, the sample with lower glass ionomer con-

Table 2
The sheet resistivity (Ω cm) as a function of the deposition time and catalyst-to-glass ratio.

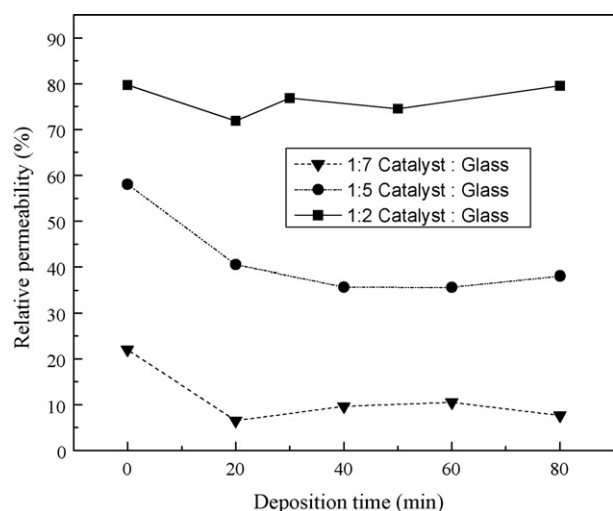| Deposition time (min)	Catalyst-to-glass ratio			
	1:2	1:4	1:5	1:7
0	1450	7250	36,500	121,000
10	801	2550	8,050	9,650
20	250	2600	6,900	7,250
30	158	2450	5,000	3,700
40	106	1350	2,200	3,800
50		733	911	6,550
60		146	237	10,300

Fig. 7. Relative methanol permeability as a function of the PtRu electroless deposition time with a different catalyst-to-glass ratio electrodes.

Fig. 8. Current density at 0.2 V (vs SCE) as a function of the PtRu electroless deposition time with a different catalyst-to-glass ratio electrodes.

tent showed lower sheet resistivity than the sample with higher ionomer content. The sample with a 1:2 catalyst-to-glass ratio showed 106 Ω cm in 40 min deposition time, while the 1:4 and 1:5 catalyst-to-glass ratios required 60 min to achieve 146 and 236 Ω cm sheet resistivity, respectively. Only the 1:7 catalyst-to-glass ratio sample did not achieve lower than 1 kΩ cm resistivity. It was observed that some of the deposited metal films delaminated, which caused an increase in the resistivity after 60 min deposition time. This could be because the metal film deposited on top of the glass ionomer was less intimately attached to the glass electrode.

The methanol blocking effect of the added, electrolessly deposited metal layer was investigated. Glass electrodes with 1:2, 1:5, and 1:7 catalyst-to-glass ratios were prepared on one side of a bare membrane. The methanol permeability of the single sided MEA was measured as a function of electroless deposition time. As seen in Fig. 7, the relative permeability of the single sided MEA decreased by more than 15% when the PtRu deposition time was 20 min. This is due to metal ions filling the void space in the catalyst layer resulting in lower methanol permeability. However, the relative permeability for both the 1:5 and 1:7 catalyst-to-glass samples did not decrease further. The additional metal film electrolessly deposited on the metal-filled glass catalyst did not change the methanol permeability. The catalyst layer of the 1:2 catalyst-to-glass sample flaked off in the acidic electroless bath, so the permeability coefficient did not decrease from the initial value. It is clear that additional glass is necessary to hold the catalyst particles on the membrane during immersion in the acidic electroless bath, when immersed for a longer time.

A decrease in methanol permeability is a benefit, if a corresponding decrease in catalytic activity does not occur when additional metal is electrolessly deposited. The effect of additional metal layers on the electrochemical activity for methanol oxidation was investigated. Fig. 8 shows the current density as a function of deposition time, ranging from 0 to 80 min. The current density was taken at 0.2 V (vs SCE) from the voltammograms obtained in 0.5 M H_2SO_4/1 M methanol solution, since it is potential range of interest for methanol oxidation in a fuel cell [24,25]. As seen in Fig. 8, the current density increased with PtRu electroless deposition time, because a greater catalyst area is available for methanol oxidation. However, the current density decreased after 60 min. The excess electroless plating decreases the actual surface area of the catalyst, making large metal islands. Evaluation of 1:2 catalyst-to-glass sample was not possible because of poor adhesion of the catalyst layer to the carbon paper due to insufficient glass in the electrode
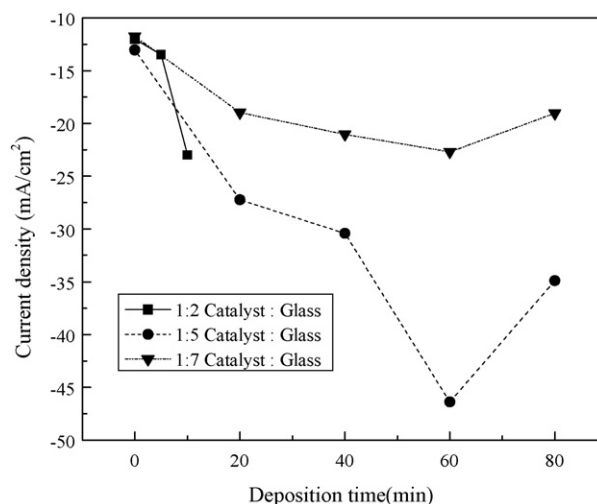
mixture. From the results shown in Table 2, Figs. 7 and 8, it is clear that the deposited metal improves three key parameters of the glass electrode, including the catalyst performance, methanol permeability, and the sheet resistivity.

The voltammetric results shown in Figs. 3, 6 and 8 are valuable in assessing the activity of the PtRu surface for methanol oxidation, however, the configuration is different from an actual fuel cell because the protons produced in the oxidation of methanol do not travel through the membrane itself. In the fuel cell, protons are produced at the catalyst surface, and travel through the ionomer in the electrode and membrane. Protons generated at the anode migrate toward the cathode through the PEM glass membrane. In order to evaluate the effectiveness of the electrodes on the membranes for use in a fuel cell, an electrode was fabricated on one side of the membrane, which was used as the working electrode of a three-electrode cell. The counter electrode was placed on the opposite side of the membrane so that the protons produced had to travel through the membrane, as they would in an operating fuel cell. The SCE reference electrode was located in the same compartment as the working electrode. A 1 M methanol solution with 0.1 M sodium sulfate was used in the anode side. The compartment on the other side of the membrane was filled with the 1 M H_2SO_4 solution. IR compensation was used to correct uncompensated resistance. The optimized, 1:5 catalyst-to-glass electrode was used as the anode. Fig. 9 compares the current densities from linear sweep voltammetry when the counter electrode is placed on the opposite side of the membrane to those from the previous experiments where the counter electrode was placed in the same compartment as the working electrode, shown in Fig. 8. When the protons had to flow through the membrane, the current density, at the same potential, and for the same electrode material, was lowered by about 50%.

A glass MEA was fabricated with an electrode on each side using the sulfonic acid-functionalized glass membrane [15] in order to test the fuel cell performance with the optimized glass anode. At the cathode, the PtRu/C was replaced with Pt/C (40 wt% metal loading) from the optimized glass anode. After curing both electrodes at 80 °C for 12 h, the PtRu and Pt were electrolessly deposited on the anode and cathode, respectively. Fig. 10 shows the polarization curve for a passive fuel-delivery DMFC operated at room temperature with 0.5 M methanol in the anode compartment and ambient air at the cathode without circulation at either electrode. The open-circuit voltage was 476 mV and the current density at 400 mV was 236 μA cm^{-2}. The fuel cell life time-test was performed at constant voltage, 400 mV, shown in Fig. 11. The current density was ca.
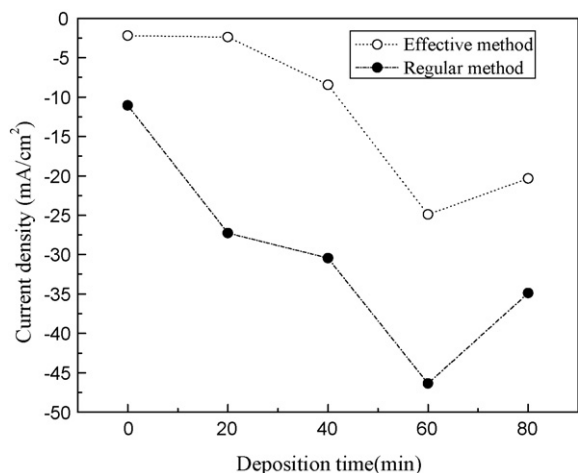
Fig. 9. Current density at 0.2 V (vs SCE) evaluated with more effective method as a function of the PtRu electroless deposition time with a 1:5 catalyst-to-glass ratio electrode, compared to the previous method.
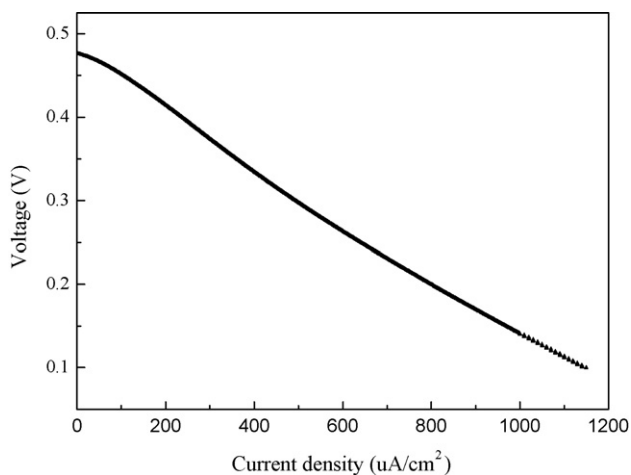

Fig. 10. A linear polarization curve for a fully passive DMFC with a glass membrane and glass electrodes; 23 °C, 0.5 M methanol, 1 mV s^{-1}.
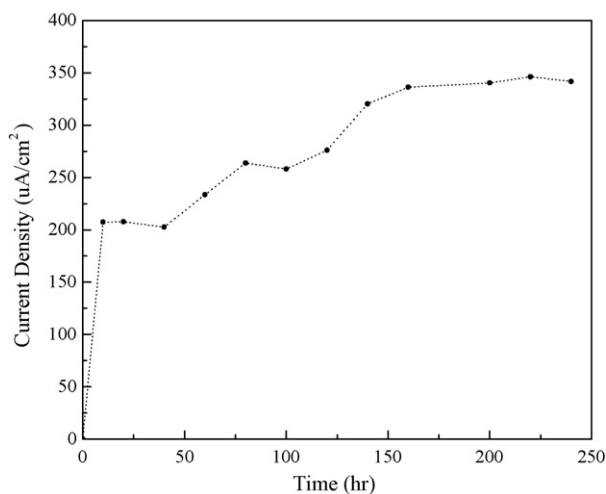

Fig. 11. Life time-test for a fully passive DMFC with a glass membrane and glass electrodes at 0.4 V; 23 °C, 0.5 M methanol.

200–250 μA cm^{-2} for the first 100 h, and increased to 340 μA cm^{-2} and remained constant thereafter.

4. Conclusion

Inorganic glass electrodes have been synthesized via a sol–gel reaction using 3TPS and GPTMS, by incorporating the PtRu/C nanoparticles into a silicon dioxide matrix. The effect of the gelation time, curing temperature, the mole ratio of the sol components, and the ratio of catalyst-to-glass in the electrode were investigated. The optimized glass electrode was obtained at the following conditions: 90% of 3TPS, a reaction time of 3 h, and curing at 80 °C. PtRu layer was electrolessly deposited on top of the glass electrode as a current collector. It was found that the optimum electroless deposition time was 60 min. The methanol permeability and the catalytic activity of the electrodes for methanol oxidation were improved. The inorganic MEA showed stable performance for more than 10 days.

Acknowledgements

References

[1] S.K. Kamarudin, W.R.W. Daud, S.L. Ho, U.A. Hasran, Journal of Power Sources 163 (2007) 743.
[2] V. Neburchilov, J. Martin, H. Wang, J. Zhang, Journal of Power Sources 169 (2007) 221.
[3] S. Prakash, W. Mustain, P.A. Kohl, Journal of Power Sources 185 (2008) 392.
[4] S. Prakash, Ph.D. thesis, Georgia Institute of Technology, 2009.
[5] W.M. Qian, D.P. Wilkinson, J. Shen, H.J. Wang, J.J. Zhang, Journal of Power Sources 154 (2006) 202.
[6] Y.S. Park, Y. Yamazaki, European Polymer Journal 42 (2006) 375.
[7] S.Z. Ren, G.Q. Sun, C.N. Li, S.Q. Song, Q. Xin, X.F. Yang, Journal of Power Sources 157 (2006) 724.
[8] C.Y. Yen, C.H. Lee, Y.F. Lin, H.L. Lin, Y.H. Hsiao, S.H. Liao, C.Y. Chuang, C.C.M. Ma, Journal of Power Sources 173 (2007) 36.
[9] R.C. Jiang, H.R. Kunz, J.M. Fenton, Journal of Membrane Science 272 (2006) 116.
[10] S. Prakash, W.E. Mustain, S. Park, P.A. Kohl, Journal of Power Sources 175 (2008) 91.
[11] C. Wang, Y. Abe, T. Kasuga, M. Nogami, Journal of the Ceramic Society of Japan 107 (1999) 1037.
[12] T. Uma, K. Hattori, M. Nogami, Ionics 11 (2005) 202.
[13] S. Sakka, H. Kozuka, Journal of Sol–Gel Science and Technology 13 (1998) 701.
[14] D.A. Ward, E.I. Ko, Abstracts of Papers of the American Chemical Society 209 (1995) 182.
[15] S.P. Hyea Kim, E. William, Mustain, A. Paul, Kohl, Journal of Power Sources 193 (2009) 562.
[16] W.E. Mustain, H. Kim, S. Prakash, J. Stark, T. Osborn, P.A. Kohl, Electrochemical and Solid State Letters 10 (2007) B210.
[17] F.H. Leaman, Plating 59 (1972).
[18] F.H. Leaman, U.S. Patent Editor, 1972.
[19] W.E. Mustain, H. Kim, T. Osborn, P.A. Kohl, Israel Journal of Chemistry 48 (2008) 251.
[20] S.W. Li, M.L. Liu, Electrochimica Acta 48 (2003) 4271.
[21] G. Alberti, M. Casciola, R. Palombari, A. Peraio, Solid State Ionics 58 (1992) 339.
[22] J.S. Lee, K.I. Han, S.O. Park, H.N. Kim, H. Kim, Electrochimica Acta 50 (2004) 807.
[23] E. Passalacqua, F. Lufrano, G. Squadrito, A. Patti, L. Giorgi, Electrochimica Acta 46 (2001) 799.
[24] S. Wasmus, A. Kuver, Journal of Electroanalytical Chemistry 461 (1999) 14.
[25] T. Iwasita, Electrochimica Acta 47 (2002) 3663.